International Journal of GEOMATE, April, 2025 Vol.28, Issue 128, pp.141-148
ISSN: 2186-2982 (P), 2186-2990 (O), Japan, DOI: https://doi.org/10.21660/2025.128.s8657
Geotechnique, Construction Materials and Environment

EVACUATION RISK ASSESSMENT ON FLOODING SLOPING ROAD DURING TYPHOON HAGIBIS AND PAST DISASTERS IN KAMAISHI

* Yuriko Matsubayashi [1] and Mako Ebina [2]

[1] Faculty of Science and Engineering, Iwate University, Japan; [2] Aomori prefecture, Japan,

*Corresponding Author, Received: 23 Jan. 2025, Revised: 27 Feb. 2025, Accepted: 28 Feb. 2025

ABSTRACT: With increasing heavy precipitation due to climate change, it is crucial to quantitatively assess flood risk. During Typhoon Hagibis, which lasted from the 12th to the 13th of October 2019, flooding obstructed evacuation routes. Studies have been conducted to evaluate the evacuation risk of flooded roads. However, a comprehensive risk assessment of flooded sloping roads has not been reported. This study aims to establish a method to estimate the risk of evacuation on flooded, water-flowing slopes. The predicted hazard and inundated areas from past disasters are shown in the hazard map of Kamaishi City. This study presents a risk evaluation of pedestrian evacuation on slopes utilizing the fluid force calculated using the estimated velocity and water depth for the maximum rainfall due to Typhoon Hagibis. The velocity and water depth were estimated using rational runoff and velocity formulae. Consequently, more than 30% of the 86 sloping roads described in the hazard map were determined to be unsuitable as evacuation routes, and a positive correlation was observed between risk and upstream areas. A simple evacuation risk assessment of a sloping road with water flow can be performed by calculating the fluid force using the estimated velocity and water depth.

Keywords: Pedestrian evacuation risk assessment, Flooding sloping road, Fluid force and Typhoon Hagibis

1. INTRODUCTION

On the 12th of October 2019, Hagibis made landfall on the Izu Peninsula in Shizuoka Prefecture, Japan. Subsequently, Hagibis made its way northward and weakened to an extratropical cyclone by 12 a.m. on the 13th.

Heavy rain induced by Hagibis caused heavy damage, particularly in the Kanto and Tohoku regions of Japan. Kazama *et al.* [1] and Enomoto *et al.* [2] reported the results of a survey and analysis of the disaster caused by typhoons Hagibis. A total of 91 people were killed by flood and sediment disasters, and three people were reported missing. In the Iwate Prefecture, at the Fudai forecast point in the northern area of Iwate, rainfall of 95.0 mm per hour was recorded. Three people were killed and seven were injured by Hagibis [3].

We conducted a survey interview of residents of the Iwate Prefecture. Survey results showed that people were exposed to danger during evacuation. These risks could have been avoided through better disaster risk assessment and evacuation actions.

Disaster prevention measures need to be planned considering the terrain, disasters, and characteristics and resources of each region. Kunsuwan *et al.* [4] used simulations to study better evacuation methods from landslides and floods in hilly areas of Thailand. Tang *et al.*[5] clarified the evaluation criteria and their overview for high-risk slopes, and through the workshop, they clarified the structure of residents' anxiety regarding slopes and strengthened self-help to evacuate using the installed tilt meters. In this study, we establish a method to estimate the risk of evacuation on flooded water-flowing slopes to properly evaluate road hazards, such as those observed in Kamaishi City during Typhoon Hagibis, and to suggest better disaster prevention.

In Touni, Kamaishi (Fig. 1), several evacuees were obstructed by the water flow on a sloping road. As shown in Fig. 2, the sloping road is an evacuation route to the Touni elementary and junior high schools, which are designated as evacuation shelters and refuge places.

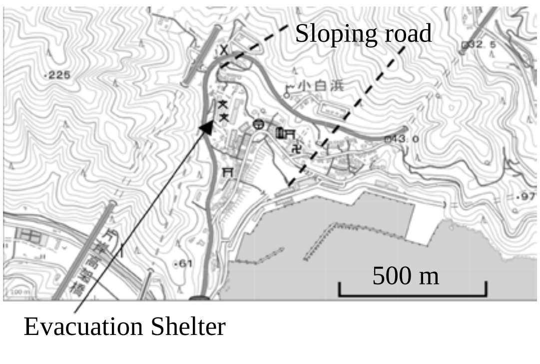

Fig. 1 Sloping road at the town of Touni. Arrows and text are added to the map [11].

At approximately 10 a.m. on the 13th of October, 2019, the sloping road was inundated. As the water flows over evacuation route, some residents could not reach the evacuation shelter.

In Kamaishi, a geographic information system (GIS) hazard map has been published online. The hazard map shows predicted floods, sedimentary disasters, tsunamis, hazards, and designated evacuation shelters and refuge places [10]. The map also shows past disasters caused by heavy rain. Information on past disasters was collected from residents. The map also shows the numerous sloping roads over which water or debris had flown during past heavy rain disasters.

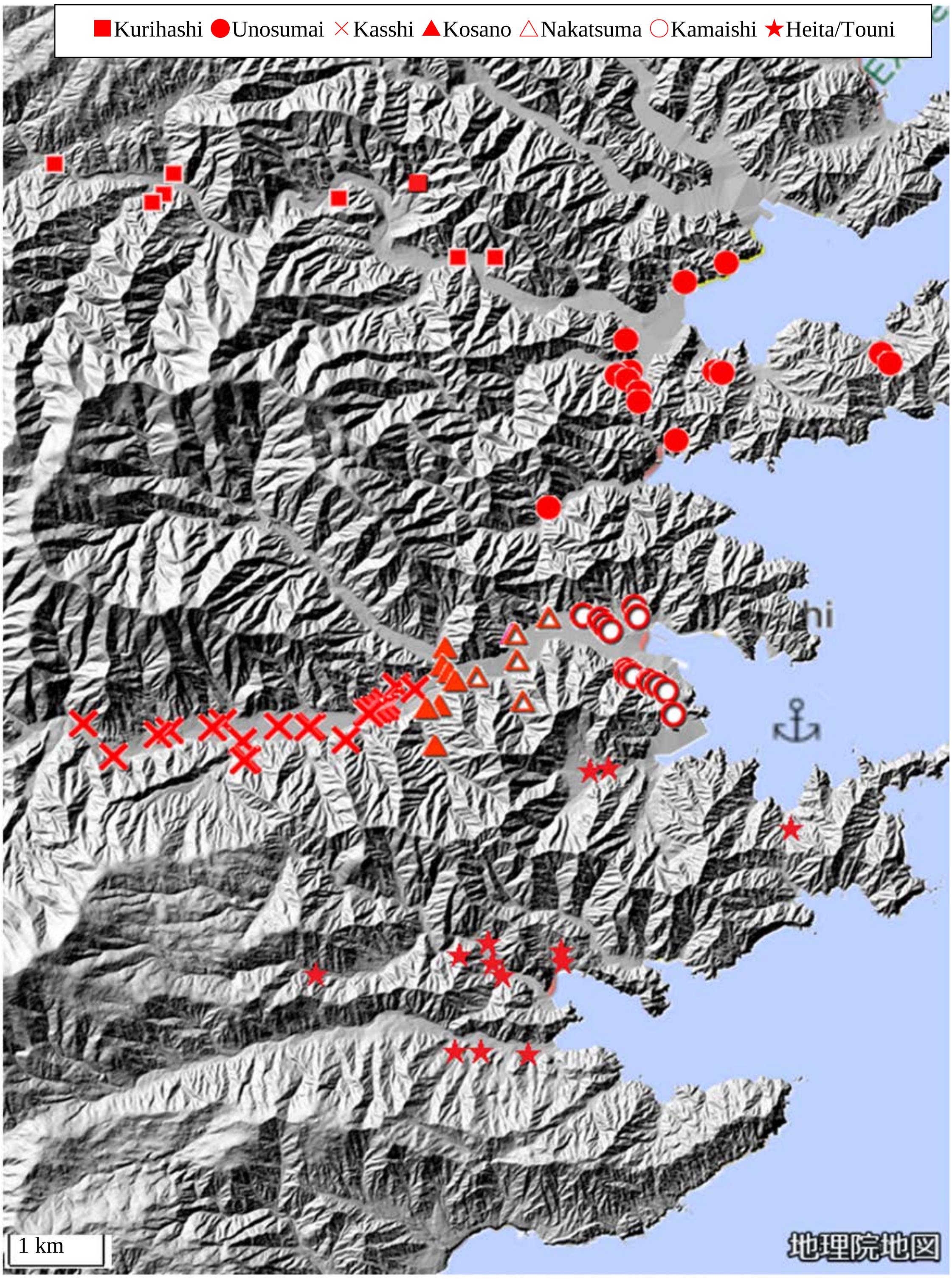

Fig. 2 Location of extracted roads in seven areas. Markers and dot lines are drawn on the map [11]

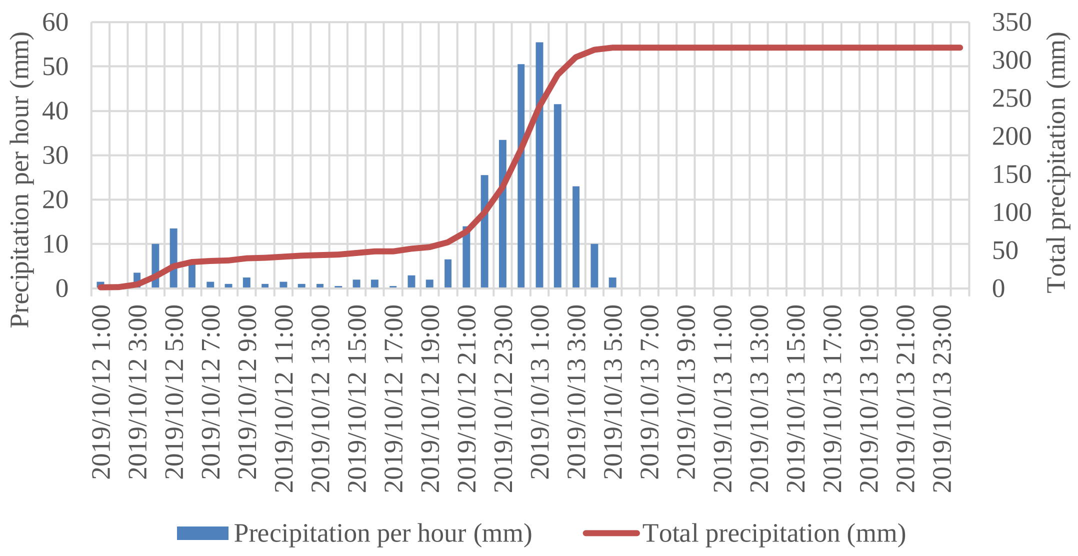

Fig. 3 AMeDAS rainfall at the Kamaishi station (12^{th}–13^{th} of October 2019) [13]

Figure. 2 shows the location of the roads, and the danger of sloping roads in Touni is indicated in the hazard map as past disaster information; nevertheless, the evacuees were exposed to danger.

Evacuation under flooding conditions is affected by the water depth and velocity. Suga *et al.* [6] investigated the safety threshold of water depth and velocity and proposed an evaluation index using the fluid force, buoyant power, and friction force [6]. Asai *et al.* [7] used the specific power to calculate a safety index for evacuation. Dias *et al.* [8] and Lee *et al.* [9] conducted experimental studies on human walking behaviors under inundation conditions.

Although studies have examined evacuation during flooding, little is known about the danger of walking on sloping roads in such conditions. In this study, we assessed the evacuation risk using the estimated water depth and velocity calculated using runoff volumes, slope, and road width. We extracted roads that indicated past inundation from the hazard map for Kamaishi. Precipitation data at the Kamaishi station of AMeDAS [13] from the 12^{th} to the 13^{th} of October 2019 were used for the estimation. The precipitation data are presented in Fig. 3. We identified various causes for inundation and water flow over sloping roads. We then categorized the roads by cause and determined the catchment areas to calculate runoff volumes in the catchment basin. The results indicated that 30% of the roads shown as flooded in the past were at risk of being impassable during heavy rains.

2. RESEARCH SIGNIFICANCE

In Japan, flooding disasters are mitigated by anti-flood control and river improvement measures for rivers managed by the government and prefectures. Flooding predictions for these rivers have been published, along with their associated hazards. However, small rivers, streams, and the causes of inland flooding managed by municipalities are not managed or predicted, similar to large rivers. Flooding on sloping roads is a part of inland inundation; however, it can be a life-threatening danger for evacuees. This study presents the results of a risk assessment of pedestrian evacuation on sloping roads during flooding.

3. METHOD

We extracted 86 roads that have been flooded in the past from the hazard map. Figures 4 and 5 show an example of a road in the Nakatsuma area and a catchment area, respectively. The gradation shows elevation. The locations of the targeted roads in seven areas (Unosumai, Kurihashi, Nakatsma, Kasshi, Kosano, Kamaishi, and Hirata/Touni) are shown in Fig. 2. These seven areas are administrative districts in the city of Kamaishi. Each area has unique geographical characteristics. The Unosumai area includes the lower reaches of the Unosumai River and Cape, whereas the Kurihashi area lies in the upper reaches of the Unosumai River. The Kasshi, Nakatsuma, Kosano, and Kamaishi areas are located along the Kasshi River.

Most houses have been built on the floodplain of the Kasshi River or steep slopes along tributary rivers. The Hirata/Touni area is located south of the city. Houses have been constructed along small rivers and hills.

All targeted roads were paved with asphalt. The roads contain gutters for drainage, streams flowing along the roads, and culverts installed under the roads.

The roads were categorized by area, number of houses along the road, and cause of flooding. The road specifications, length, width, elevation slope, number of houses along the roads, and detour routes for evacuation were calculated using a GIS map [11]. Table 1 lists the number of categorized roads.

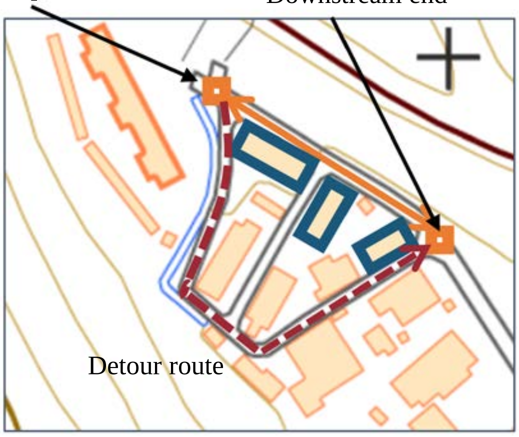

Fig. 4 Example of a sloping road and detour route. Markers and dot lines are drawn on the map [11].

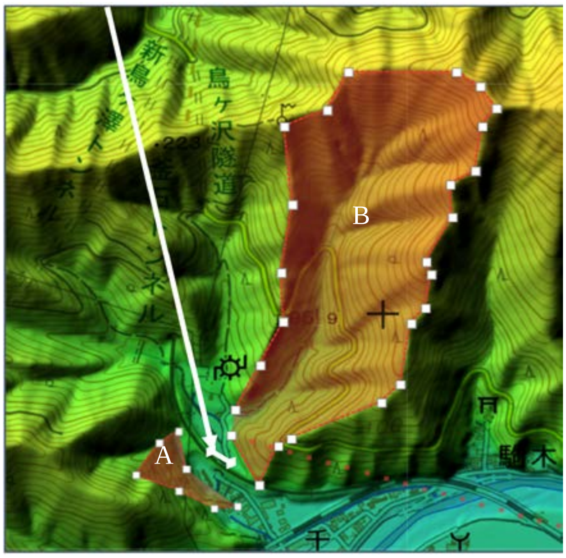

Fig. 5 Example of catchment area. Markers and dot lines are drawn on the map [11].

A road without a catchment area is inundated by the Kasshi River flooding or has poor drainage. A road without a house has a low probability of being used for evacuation. For the 86 roads, the overflow of streams along the road or culverts under the road mainly caused the flooding. With heavy rainfall, higher flow rates or clogging by debris increases the water elevation; therefore, overflowing water floods roads. Hence, in this study, we consider the predicted runoff volume of streams along or under a road as the flow rate of water volume flowing over the road.

Table 1. Road numbers in areas

Area name	Total	No catchment area	No house
Unosumai	14	0	2
Kamaishi	15	0	1
Heita/Touni	13	1	4
Kurihashi	8	1	3
Kasshi	23	7	1
Nakatsuma	6	1	0
Kosano	7	3	0
Total	86	13	11

In the example of Touni (Fig. 1), a river flowing under the road is clogged by water flowing over the road. Owing to steep slope of the road, water runs down at high speeds; thus, evacuees are hindered from evacuating.

3.1 Velocity and Water Depth on The Roads

The evacuation risk for each road was indicated in two methods using the estimated velocity and water depth on the roads.

The velocity and depth of the water flow on the roads were estimated using the runoff volume calculated and rational formulae (Eqs. (1), (2), and (3)) using the catchment area and precipitation data (Fig. 4) [12].

$$Q = 1/3.6 \times f \times r \times A \quad (1)$$

$$t = 30\sqrt{A}/\sqrt{2} \quad (2)$$

$$T = 1/3600 \times L/W \quad (3)$$

Here, Q, f, r, A, t, and T denote the flow rate, discharge coefficient, design rainfall intensity, catchment area, inlet time, and flow time, respectively. The time of concentration is the summation of $t + T$; L denotes the length of the river channel from its outlet point to its farthest point, and W refers to the flow velocity obtained using Kraven's formula.

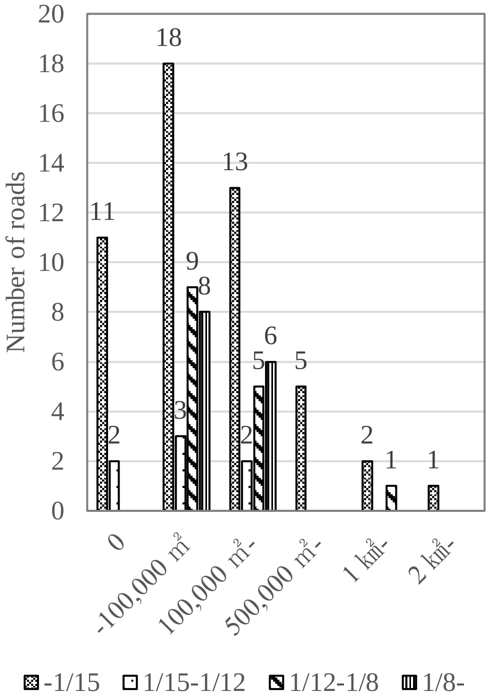

Fig. 6 Catchment area and road slope

We obtained the velocity and water depth for a rectangular channel using Manning's formula (Eqs. (4) and (5)) under the assumption that the roads are wide rectangular channels with a constant width and slope.

$$v = Q/bh = (1/n) \times R^{\frac{2}{3}} \times i^{\frac{1}{2}} \tag{4}$$

$$h = \left(nQ/bi^{\frac{1}{2}}\right)^{\frac{2}{5}} \tag{5}$$

Here, v, b, n, R, and i denote the flow velocity, width of the road, Manning's roughness coefficient, hydraulic radius, and slope, respectively. Considering roads are considered very wide channels, we regarded R as h.

3.2 Assessment of Evacuation Risk

We compared the results of the risk assessment obtained by comparing the fluid and resistance forces [6] with the specific force per unit width [7].

3.2.1 Comparison between fluid force and resistance force

Suga *et.al.* [6] compared the fluid and resistance forces (hereinafter called $2D - F$) to evaluate the risk of walking under a water flow. The fluid force is calculated using Eq. (6). The resistance force, calculated using Eq. (7), is the friction force between the sole of the shoe and the ground. Equation (8) is the criterion. We added terms that consider the slope effect to the equations described by Suga *et al.* [6].

$$D = C_d \times \{\rho(u+v)^2 \times a/2\} + G_0 \sin i \tag{6}$$

$$F = f \times (G_0 \sin i - W) \tag{7}$$

$$F \geq \alpha D \tag{8}$$

Here, D, C_d, ρ, u, a, G_0, F, W, and α denote the fluid force, drag coefficient for the human body, density of water, walking speed (0.4 m/s in this study), projected area of the human body, body weight (60 kg × 9.8 m/s^2 in this study), resistance force, buoyant force, and safety factor, respectively. In this study, α was set to 2 following Suga *et. al.* [6]

3.2.2 Specific force per unit width

We calculated the specific force per unit M (hereinafter referred to as M) using Eq. (9) to evaluate the risk of walking under flooding conditions, following Asai *et. al.* [7]. Asai *et al.*[7] conducted walking experiments in a waterway to obtain threshold values for the specific force per unit width during evacuation by gender and age. Using these threshold values, they conducted simulations from flooded underground spaces to obtain risk assessment of the evacuation route. The simulations combined changes in flooding status over time based on simulation calculations and evacuees' behavior by gender and age.

$$M = (v^2h/g) + (h^2/2) \tag{9}$$

Here, g represents the gravitational acceleration. Table 2 specifies the criteria of M classified for men in their twenties, women in their twenties, elderly men, and elderly women, as proposed by Asai *et. al.* [7]

Table 2. Criterion of specific force per unit width [7]

	Safe for evacuation	Obstruction from flooding
Male 20s	$\boldsymbol{M < 0.125}$	$\boldsymbol{M > 0.250}$
Female 20s / Male senior	$\boldsymbol{M < 0.100}$	$\boldsymbol{M > 0.200}$
Female senior	$\boldsymbol{M < 0.080}$	$\boldsymbol{M > 0.160}$

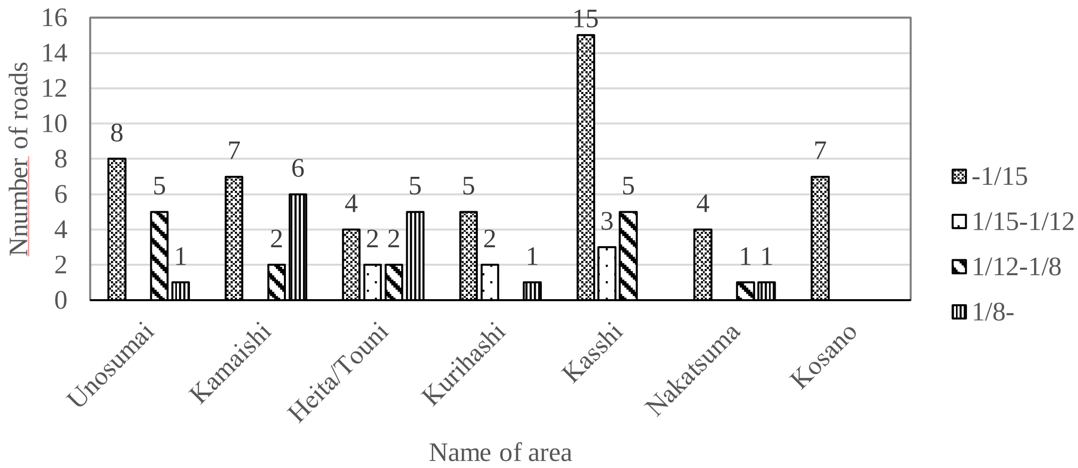

Fig. 7 Road slope in each area

Table 3. Result of evacuation risk assessment

	water depth > 0.3m	Comparison between fluid force and resistance force	specific force per unit		
			M > 0.123	M > 0.100	M > 0.08
Unosumai	1	8	8	9	10
Kamaishi	1	4	4	4	5
Heita/Touni	1	7	7	7	8
Kurihashi	0	3	5	5	5
Kasshi	1	2	3	4	4
Nakatsuma	0	3	3	3	4
Kosano	1	1	1	1	2
total	5	28	31	33	38

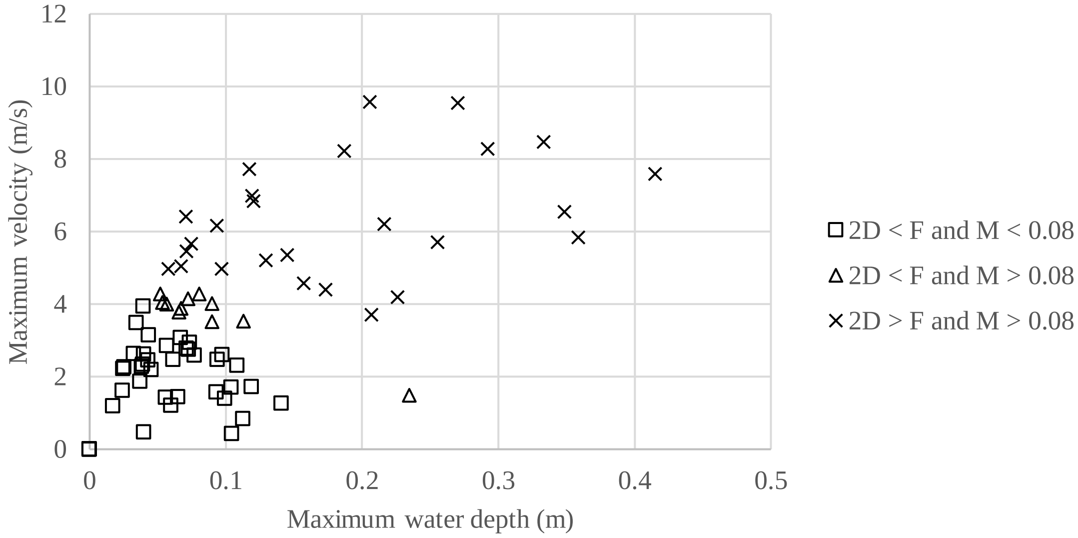

Fig. 8 Maximum velocity, maximum water depth, and assessment results

4. RESULTS

Catchment area and road slope are crucial aspects of flow conditions. Figure. 6 depicts the relationship between the catchment area and road slope. In Japan, the development standards for steep slopes have been legally established. For wheelchairs, the installation criterion for slopes in public spaces has been determined. A sloping path steeper than 1/12 requires arm rails on both sides of the path. The sloping path, instead of stairs in buildings, must be milder than 1/8 [14].

As shown in Fig. 6, most roads were milder than 1/15 and had small catchment areas. A 1/15 slope is sufficiently gentle for walking under dry conditions; however, it is as steep as a river slope. Figure. 2 shows that the target roads included numerous roads laid along or over steep rivers or mountain streams.

Figure 7 presents the road slopes to compare the characteristics of each area. In the Kasshi area, 15 of the 23 roads were milder than 1/15. Although the roads are gentle, water flow from the catchment area located on steep slopes on both sides of the Kasshi River induces flooding.

Table 3 presents the results of the risk assessment with water depth, $2D-F$, and M values for each area. In most hazard maps, a water depth of 0.3 m—below knee level—is considered the threshold depth for safe pedestrian evacuation. The assessment results differ for each method. The estimated water depth was sufficiently low for on-foot evacuation under flood conditions on most of the targeted roads. However, the assessment using $2D-F$ indicated that 28 roads were considered unsafe for on-foot evacuation.

With the assessment using M, 38 of 86 roads were considered unsafe for the on-foot evacuation of elderly women. The roads in Touni (Fig. 2) were safely assessed in terms of the water depth, but not by $2D-F$ and M.

We compared the assessment results with $2D-F$ and M. Figure 8 depicts the relationship between the maximum velocity and maximum water depth for each road. The roads were categorized based on the results of the two risk assessment methods, $2D-F$ and M. Figure 8 shows that the criterion of M is stricter than that of $2D-F$. Outlier data are excluded from Fig. 8. The maximum velocity and maximum water depth of the excluded road are 15.1 m/s and 0.72 m, respectively, because the catchment area is larger than that of others. In addition, the Kasshi area had roads with outlier data and were not safe for risk assessment using $2D-F$ and M.

5. DISCUSSION

This study presents the results of a risk assessment of on-foot evacuation under flooding conditions in Kamaishi City. The assessment was performed on roads extracted from the hazard map. This study introduces a simple method to assess the evacuation risk of sloping roads in catchment areas. The results show the difference between the assessment method and evaluated disaster scales of the evacuation route.

Therefore, for the risk assessment of inland flooding and publishing hazard maps, it is recommended to establish the cause of flooding and effect of sloping roads to adequately estimate the risk. However, owing to the work cost and small disaster scale, only a few hazard maps present accurate disaster predictions for inland flooding. Considering the assessment in this study was based on assumptions concerning the estimation of the flow rate over roads, further studies are needed to enhance accuracy.

6. CONCLUSION

In Kamaishi, roads flooded during past disasters were shown on a hazard map. Numerous flooded roads slope with streams along or beneath them. The on-foot evacuation risk of roads under heavy rain conditions was estimated under the assumption that these inland flooding events are caused by overflowing rivers, streams, or culverts along or under each road. The results revealed differences between the assessment results of each assessment method.

7. ACKNOWLEDGMENTS

The authors would like to thank all members of the construction division of Kamaishi City Hall for their helpful suggestions and approval of the survey. We would like to thank Editage for editing and reviewing this manuscript for English language.

8. REFERENCES

[1] Kazama M., Yamakawa Y., Yamaguchi A., Yamada S., Kamura A., Hino T., and Moriguchi S., Disaster Report on Geotechnical Damage in Miyagi Prefecture, Japan caused by Typhoon Hagibis in 2019. Soils and Foundations, Vol. 61, Issue 2, 2021, pp. 549–565.

[2] Enomoto T., Horikoshi K., Ishikawa K., Mori H., Takahashi A., Unno T., and Watanabe K., Levee Damage and Bridge Scour by 2019 Typhoon Hagibis in Kanto Region, Japan. Soils and Foundations, Vol. 61, Issue 2, 2021, pp.

566–585.
[3] Iwate prefecture, Disaster Information Portal, https://iwate-bousai.my.salesforce-sites.com/PUB_VF_TopA, in Japanese.
[4] Kunsuwan N. and Kunsuwan B, Management Guidelines For Evacuation Routes in Areas Prone to Flooding and Landslides: a Cace Study of the Mae Phrong River Basin Area in Thailand, International Journal of GEOMATE, Vol.21, Issue 88, 2021, pp.97-104.
[5] Tang Z., Miyamoto Y., Oji S., and Fujitani H., Resident Participatory Monitoring of Slope Disasters Using Tilt Sensors, International Journal of GEOMATE, Vol. 25, Issue 108, 2023, pp.114-121.
[6] Suga K., Uesaka T., Yoshida T., Hamaguchi K., and Chen Z., Preliminary Study on Feasible Safe Evacuation in Flood Disaster, Annual Journal of Hydraulic Engineering, JSCE, Vol. 39, 1995, pp. 879–882, in Japanese.
[7] Asai Y., Ishigaki T., Baba Y., and Toda K., Safety Analysis of Evacuation Routes Considering Aged Persons During Underground Flooding, Annual Journal of Hydraulic Engineering, JSCE, Vol. 53, 2010, pp. 859–864, in Japanese.
[8] Dias C., Rahman, N. A., and Zaiter, A., Evacuation Under Flooded Conditions: Experimental Investigation of the Influence of Water Depth on Walking Behaviors, International Journal of Disaster Risk Reduction, Vol. 58, 2021, 202192.
[9] Lee Won H.K. and Youn-Ha Lee H.H, Experimental Study on the Influence of Water Depth on the Evacuation Speed of Elderly People in Flood Conditions, Elsevier, International Journal of Disaster Risk Reduction, Vol. 39, 2019, 101198.
[10] The City of Kamaishi, Kamaishi City Floods and Landslide Hazard Map, https://kamaishi.nigedoki-map.com/, in Japanese.
[11] Ministry of Infrastructures, Transport and Tourism Geospatial Information Authority of Japan, GIS Maps, https://maps.gsi.go.jp, in Japanese
[12] Kagoshima Prefecture, Design Criteria of River Works https://www.pref.kagoshima.jp/ah07/infra/kasen-sabo/kasenseibi/sekkeikijyun.html, in Japanese.
[13] Japan Meteorological Agency, https://www.data.jma.go.jp/stats/etrn/index.php.
[14] Order of Ministry of Land, Infrastructure, Transport and Tourism, https://laws.e-gov.go.jp/law/418M60000800114/, in Japanese.